



ELSEVIER

Nuclear Instruments and Methods in Physics Research B 141 (1998) 461–466

NIM B
Beam Interactions
with Materials & Atoms

Radiation effects in corundum structure derivatives

J.N. Mitchell ^{a,*}, R. Devanathan ^b, N. Yu ^c, K.E. Sickafus ^a, C.J. Wetteland ^a,
V. Gopalan ^a, M.A. Nastasi ^a, K.J. McClellan ^a

^a Materials Science and Technology Division, Los Alamos National Laboratory, Mail Stop K762, Los Alamos, NM 87545, USA

^b Pacific Northwest National Laboratory, Richland, WA 99352, USA

^c Texas Instruments, Inc., Dallas, TX 75243, USA

Abstract

The radiation response of α -Al₂O₃ ($R\bar{3}c$), FeTiO₃ ($R\bar{3}$), MgTiO₃ ($R\bar{3}$), and LiTaO₃ ($R3c$) was investigated using 200 keV Ar²⁺ and 1 MeV Kr⁺ and a combination of Rutherford backscattering spectrometry and transmission electron microscopy. All of these materials have the corundum or a corundum-derivative crystal structure. This family of oxides is of interest due to the simple but significant differences in the structure of the cation sublattices in the different space groups. These materials are also of interest because of their range of melting temperatures, the range of melting temperatures of their oxide components, differences in bonding characteristics, and the complete solid solution between FeTiO₃ and MgTiO₃. Our results show that α -Al₂O₃ and MgTiO₃ are consistently more radiation tolerant than FeTiO₃ and that LiTaO₃ amorphizes substantially easier than the other three oxides. The greater stability of MgTiO₃ than FeTiO₃ appears to be analogous to the response of Mg-Fe silicates to ion irradiation and high pressure. A characteristic consistent with the radiation tolerance trend of the four oxides studied is a decreasing melting temperature of the component oxides. Thus, the lower stability of Fe–O octahedra in FeTiO₃ and Li–O octahedra in LiTaO₃ may adversely affect the radiation tolerance of these oxides. © 1998 Elsevier Science B.V. All rights reserved.

PACS: 61.80.Jh; 61.82.Ms; 61.85.tp

Keywords: Radiation damage; Amorphization; Corundum structure; Rhombohedral oxides

1. Introduction

Although a number of oxides have rhombohedral crystal structures, few materials except those with the corundum structure ($R\bar{3}c$) have been studied for their radiation tolerance. In particular,

sapphire (α -Al₂O₃) has been investigated extensively for use in high-radiation environments, though significant swelling in samples irradiated at high temperatures indicates that it is not well suited for reactor and accelerator applications (e.g., [1]). In contrast, magnesium aluminate spinel (MgAl₂O₄) is remarkably resistant to a variety of irradiation conditions. The superior radiation response of spinel as compared to sapphire and similar single-cation oxides has been attributed to two

* Corresponding author. Tel.: +1 505 665 3934; fax: +1 505 665 3935; e-mail: jeremy@lanl.gov.

factors: compositional complexity and the capacity for cation disorder [2]. Compositional complexity acts to suppress the nucleation and growth of dislocation loops and voids, and cation disorder is believed to facilitate the annihilation of point defects by the recombination of interstitials and vacancies. A lack of radiation damage studies on other materials with these characteristics has made it difficult to extend these two factors toward a general understanding of the radiation tolerance of multiple-cation oxides.

In this paper, we describe the results of our ongoing research into the radiation response of a variety of materials with crystal structures that are derivative of the corundum structure. In particular, this research has focused on α - Al_2O_3 ($R\bar{3}c$, corundum structure), FeTiO_3 ($R\bar{3}$, ilmenite structure), MgTiO_3 ($R\bar{3}$, ilmenite structure), and LiTaO_3 ($R3c$, lithium niobate structure). These materials are of particular interest due to the simple but significant differences in their crystallography. The basic corundum structure ($R\bar{3}c$) is composed of nearly hexagonal close-packed oxygen layers alternating with disordered octahedral cation layers perpendicular to the c -axis. In the ilmenite structure ($R\bar{3}$), the cations order in alternating layers that are separated by an oxygen layer. Each cation layer in lithium niobate-structure materials ($R3c$) consists of equal proportions of both cations. These four rhombohedral oxides are also of interest because of their range of melting temperatures, the range of melting temperatures of their oxide components, and differences in bonding characteristics (Table 1).

2. Experiments and results

Two types of experiments were used to investigate the radiation response of rhombohedral oxides in this study. Bulk single crystals were irradiated with 200 keV Ar^{2+} and damage was monitored using Rutherford backscattering spectrometry and ion channeling (RBS/C) at the Ion Beam Materials Laboratory (IBML) at Los Alamos National Laboratory. Additionally, thin foils of single crystals were irradiated in situ with ions (1 MeV Kr^+) and electrons (0.9 MeV) at the High Voltage Electron Microscope (HVEM) Tandem Facility at Argonne National Laboratory. Details of these and related experiments are described in [3–5]. The Monte Carlo code TRIM 96 [6] was used to estimate ion range and damage parameters for the two types of experiments.

2.1. 200 keV Ar^{2+} irradiations

Ion irradiations of bulk single crystals of α - Al_2O_3 , FeTiO_3 , MgTiO_3 , and LiTaO_3 were performed using 200 keV Ar^{2+} and irradiating to fluences of 1×10^{15} and 2×10^{15} $\text{Ar}^{2+}/\text{cm}^2$ while the samples were held at a temperature of 100 K. The samples were tilted by 10° from the c -axis during the irradiations to minimize channeling effects. One section of each crystal was masked from the ion irradiation and used for ion channeling alignment following the irradiations. Unirradiated and irradiated regions of the crystal were analyzed with RBS/C along the $\langle 0\ 0\ 1 \rangle$ axis using a 2 MeV He^+ ion beam. Random spectra were collected by rock-

Table 1
Physical properties of selected rhombohedral oxides

	Al_2O_3	FeTiO_3	MgTiO_3	LiTaO_3
Space group	$R\bar{3}c$	$R\bar{3}$	$R\bar{3}$	$R3c$
Lattice parameters:				
a (Å)	4.763	5.088	5.055	5.154
c (Å)	12.995	14.086	13.899	13.783
Density (g/cc)	3.97	4.72	3.85	7.45
Ionicity (Pauling)	0.59	0.54	0.64	0.70
Melting T (K)	2290	1640	1903	1923
Melting T of oxides (K)	2290	FeO 1369 TiO ₂ 1825	MgO 2852 TiO ₂ 1825	Li ₂ O 1726 Ta ₂ O ₅ 1872

ing the sample about 3° off the $\langle 0\ 0\ 0\ 1 \rangle$ channeling direction and are used for comparison with the aligned spectra. Minimum backscattering yield, defined as the RBS yield ratio of the aligned $\langle 0\ 0\ 0\ 1 \rangle$ spectrum to the random spectrum, was used to quantify the crystal quality of the sample surfaces. The initial high minimum yield values (10–30%) of all samples except LiTaO_3 indicate substantial residual damage in the surface layers due to mechanical polishing. The damaged layers were effectively removed by etching samples in hydrofluoric acid at room temperature for 5–10 min, as indicated by the minimum yield values of $\sim 3\text{--}6\%$ along the c -axis for etched samples.

RBS/C data for the 200 keV Ar^{2+} experiments are shown in Fig. 1. Each collection of spectra for the different materials includes (1) an aligned, (2) an irradiated and aligned, and (3) a random spectrum. The spectra for the aligned starting materials are all characterized by low RBS yields, resulting in the low minimum yield values described above. Surface peaks for the various constituent elements are indicated on the respective spectra in Fig. 1. After irradiation to $1 \times 10^{15} \text{ Ar}^{2+}/\text{cm}^2$,

the resulting spectrum from each sample has a higher RBS yield and the surface peaks for the elements increased significantly in yield. This behavior is attributed to increased disorder in the damaged region of the crystal.

For $\alpha\text{-Al}_2\text{O}_3$, the spectrum from the aligned crystal shows high dechanneling yields from the sample depth interval where the peak radiation damage appeared (Fig. 2(a)). The dechanneling yields from this depth interval are consistent with those of the random spectrum, indicating the formation of a 100 nm thick buried layer. This buried layer may be amorphous or could consist of randomly-oriented crystallites in an amorphous matrix, and we will refer to disordered layers such as this as random in the rest of the text. The nature of such layers will be studied in more detail using electron microscopy of cross-sectioned samples. The region directly overlying (i.e., at higher channels) this buried, highly disordered layer has a minimum yield of 25%. We interpret this feature as a 45 nm thick disordered, single crystal Al_2O_3 layer. TRIM calculations indicate that 200 keV Ar^{2+} at a fluence of $1 \times 10^{15} \text{ ions}/\text{cm}^2$ has a range

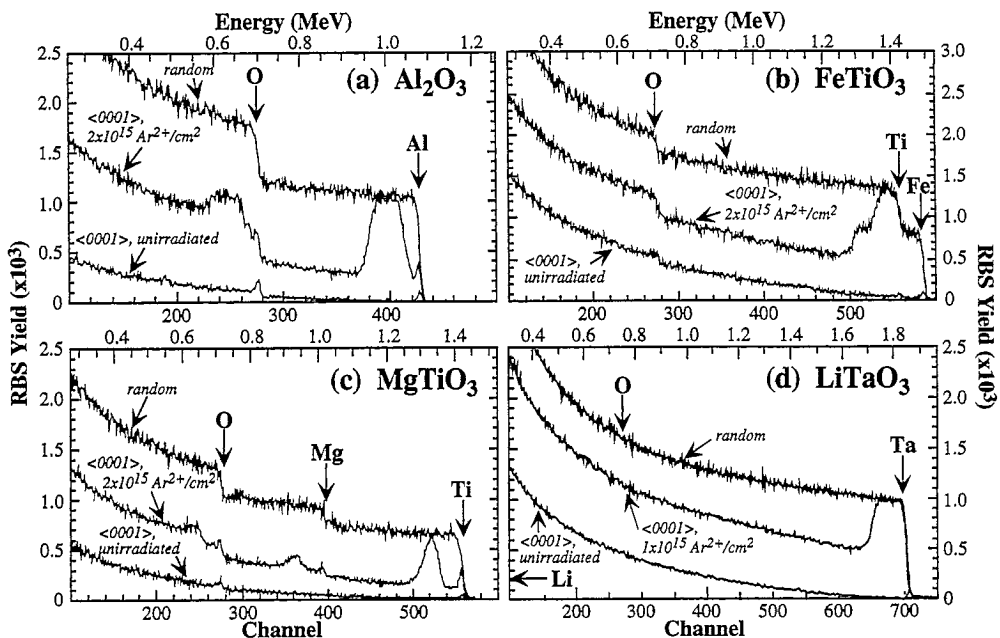


Fig. 1. RBS/C spectra for 200 keV Ar^{2+} irradiations at 100 K of Al_2O_3 (a), FeTiO_3 (b), MgTiO_3 (c), and LiTaO_3 (d). Aligned spectra are from $\langle 0\ 0\ 0\ 1 \rangle$ oriented crystals prior to irradiation and random spectra are generated by rocking the sample during RBS analysis.

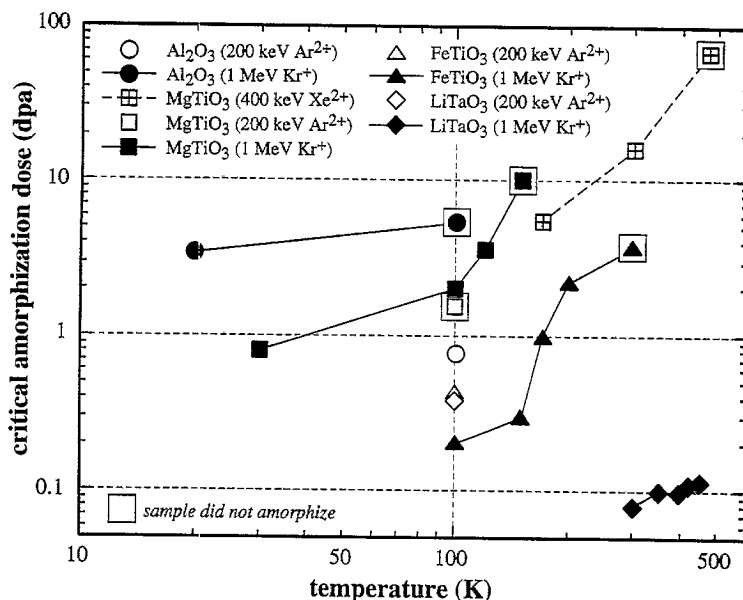


Fig. 2. Summary plot of critical amorphization dose in dpa versus temperature (K) for ion irradiation experiments conducted in this study. Also shown are data from [3] for 400 keV Xe^{2+} irradiations of MgTiO_3 . Boxes around data points indicate that the sample did not completely amorphize.

of 128 nm with a straggle of 37 nm. The damage level is 0.77 dpa in the peak damage region, where the Ar concentration is less than 0.1 at. % [6].

The post-irradiation RBS spectrum for FeTiO_3 (Fig. 1(b)) shows high dechanneling yields that correspond with a random layer 160 nm thick. The coincidence of the aligned and random spectra, particularly at the Fe edge, indicates that there is no defective crystalline layer and that the damaged region is entirely random. Electron microscopy of a cross-sectioned sample indicates that the FeTiO_3 amorphized at a fluence below $1 \times 10^{15} \text{ Ar}^{2+}/\text{cm}^2$, probably $\sim 5 \times 10^{14} \text{ Ar}^{2+}/\text{cm}^2$ [7]. Irradiation of MgTiO_3 with $2 \times 10^{15} \text{ Ar}^{2+}/\text{cm}^2$ resulted in considerable changes in the corresponding RBS spectrum (Fig. 1(c)). As with $\alpha\text{-Al}_2\text{O}_3$, a large damage peak is present between channels 500 and 540 that is adjacent to a region with lower minimum yield at higher channels. The former corresponds with a buried random-like layer 55 nm thick, whereas the latter is interpreted to be a 90 nm thick defective crystalline layer. The range and straggling of 200 keV Ar^{2+} at a fluence of $1 \times 10^{15} \text{ ions}/\text{cm}^2$ are as follows: FeTiO_3 , 127 and

44 nm; MgTiO_3 , 138 and 42 nm. The damage level and ion concentrations in the peak damage regions are 0.8 dpa and 0.1 at. % Ar for FeTiO_3 and 0.8 dpa and 0.1 at. % Ar for MgTiO_3 [6]. In Fig. 2, we have compared the results of the 200 keV Ar^{2+} irradiations with similar experiments on MgTiO_3 irradiated with 400 keV Xe^{2+} at temperatures of 170, 300, and 470 K [3]. We found that MgTiO_3 has critical amorphization doses of 5.4 and 16.2 dpa at 170 and 300 K, respectively, and that despite a peak damage region dose of 67.5 dpa, MgTiO_3 at 470 K does not amorphize.

Finally, results for irradiation of LiTaO_3 are shown in Fig. 1(d). A large damage peak is present in the RBS/C spectrum following irradiation with a fluence of $1 \times 10^{15} \text{ Ar}^{2+}/\text{cm}^2$. The damage peak in Fig. 1(d) corresponds with a random-like surface layer about 100 nm thick. At a fluence of $1 \times 10^{15} \text{ Ar}^{2+}/\text{cm}^2$, Ar has a range of 119 nm with a straggle of 51 nm and a concentration of less than 0.8 atomic % in the peak damage region. This fluence corresponds with a damage level of 0.8 dpa in the peak damage region [6]. This material damages comparatively easily and a more detailed inv-

estigation has shown that the damage rate is dependent on the internal field orientation of this ferroelectric material [8]. This study also shows that complete randomization occurs at a fluence of $\sim 5 \times 10^{14} \text{ Ar}^{2+}/\text{cm}^2$ at 100 K.

2.2. 1 MeV Kr^+ irradiations

To complement the bulk sample irradiations described above, single-crystal samples of $\alpha\text{-Al}_2\text{O}_3$, FeTiO_3 , MgTiO_3 , and LiTaO_3 were prepared as electron-transparent TEM samples and irradiated with 1 MeV Kr^+ at the HVEM-Tandem Facility. This facility consists of a 1.2 MeV modified Kratos/AEI EM7 electron microscope interfaced with two ion accelerators, and the combination of these tools provides for direct observation of microstructural changes during ion irradiation. Cooling and heating stages allow for the adjustment of sample temperatures to study the temperature dependence of the critical damage dose. In each experiment, determination of the amorphization dose was based on the complete disappearance of diffraction spots and the appearance of a halo in the diffraction pattern. Further details of these experiments are presented in [4].

Results of these irradiation experiments are similar to the 200 keV Ar^{2+} irradiations. Lithium tantalate damaged easily, requiring only 0.08 dpa to amorphize at 300 K. Increasing the temperature to 450 K increased the critical dose of amorphization to 0.115 dpa, but this material is clearly significantly less radiation resistant than the other rhombohedral oxides investigated in this study. Critical doses for amorphization at 30 K for $\alpha\text{-Al}_2\text{O}_3$, FeTiO_3 , and MgTiO_3 are 3.39, 0.19, and 0.8 dpa, respectively (Fig. 2) [4]. These results are in contrast with the 200 keV Ar^{2+} irradiations, where MgTiO_3 was found to have a radiation resistance similar to $\alpha\text{-Al}_2\text{O}_3$. Critical amorphization doses in all materials increased with increasing temperature (Fig. 2).

3. Discussion

Of the four materials examined in this study, LiTaO_3 is clearly the least radiation tolerant, fol-

lowed by FeTiO_3 . We have reported previously that the interpretation of ion-irradiation experiments on FeTiO_3 may be complicated by reduction-oxidation reactions [7]. In particular, the formation of Fe_2O_3 precipitates prior to and possibly during irradiation may compromise the radiation response of FeTiO_3 . However, no Fe_2O_3 precipitates were observed by TEM in the 1 MeV Kr^+ experiments, suggesting that our in situ irradiations are representative of the radiation response in pure FeTiO_3 rather than a $\text{FeTiO}_3\text{-Fe}_2\text{O}_3$ composite.

The FeTiO_3 and MgTiO_3 ion irradiation results are analogous to similar experiments on the olivine solid-solution system. Wang and Ewing [9] reported that Mg_2SiO_4 (forsterite) irradiated with 1.5 MeV Kr^+ is more radiation resistant than Fe_2SiO_4 (fayalite) and Fe-rich olivines in general. They attributed the greater stability of forsterite to its higher proportion of ionic bonding and higher melting temperature. Similarly, Andrault et al. [10] reported that Fe_2SiO_4 amorphizes at lower pressures than Mg_2SiO_4 . These authors attributed this behavior to the influence of (Mg, Fe) substitution on the compressibility of olivine. Most importantly, there is a lower compressibility for Mg–O octahedra than for Fe–O octahedra and the compressional anisotropy is stronger for Fe-rich olivines.

It has been suggested in several studies that a high melting temperature and a large ionic bonding component enhances the radiation tolerance of ceramics, particularly for single-cation compounds (e.g. [11]). Of the materials investigated in this study, $\alpha\text{-Al}_2\text{O}_3$ has the highest melting temperature (2290 K), followed by LiTaO_3 (1923 K), MgTiO_3 (1903 K), and FeTiO_3 (1640 K) (Table 1). In contrast, LiTaO_3 has the largest ionic component (0.70), followed by MgTiO_3 (0.64), Al_2O_3 (0.59), and FeTiO_3 (0.54) (Table 1). Alpha-alumina is the most radiation tolerant and has the highest melting temperature of these materials but has a comparatively low ionicity. Similarly, LiTaO_3 is the least radiation resistant yet has a relatively high melting temperature and a high ionic bonding component. These results contradict the observations that melting temperature and ionicity enhance radiation tolerance and suggest that other

factors may play a role in the radiation stability of multiple-cation oxides.

One factor that may enhance the relative radiation tolerance of the rhombohedral oxides examined in this study is related to the stability of cation-oxygen polyhedra in their respective structures. This is a concept related to Pauling's third rule for constructing stable structures [12], which states that shared faces and edges destabilize polyhedra and lead to distortion of the structure. The rhombohedral oxides in this study are composed of octahedra that share one face and three edges with their neighbors and are thus unstable based on Pauling's third rule. An extension of this concept is that FeTiO_3 , MgTiO_3 , and LiTaO_3 are multiple component oxides composed of two types of octahedra with different melting temperatures. For example, LiTaO_3 has a melting temperature of 1923 K, but Li_2O and Ta_2O_5 melt at temperatures of 1726 and 1872 K, respectively. Decomposition of Li–O octahedra during irradiation may destabilize the entire structure, resulting in a critical amorphization dose lower than that predicted based on the melting temperature of the bulk material. In the FeTiO_3 – MgTiO_3 system, FeO and MgO have respective melting temperatures of 1369 and 2852 K. This suggests that MgTiO_3 is more stable than FeTiO_3 , behavior that our results confirm. Though a variety of factors contribute to the radiation stability of multiple-cation ceramics, we believe that consideration of the polyhedral constituents of a material may be more valuable than trying to relate radiation response to bulk properties.

Acknowledgements

This research is sponsored by the US Department of Energy, Office of Basic Energy Sciences, Division of Materials Sciences. Additional support was provided by the Los Alamos Neutron Science Center through a Laboratory-Directed Research and Development project.

References

- [1] F.W. Clinard, Jr., G.F. Hurley, L.W. Hobbs, *J. Nucl. Mater.* 108/109 (1982) 655.
- [2] K.E. Sickafus, N. Yu, M.A. Nastasi, *Nucl. Instr. and Meth. B* 116 (1996) 85.
- [3] J.N. Mitchell, N. Yu, K.E. Sickafus, M.A. Nastasi, K.J. McClellan, *Phil. Mag.*, in press.
- [4] R. Devanathan, J.N. Mitchell, K.E. Sickafus, W.J. Weber, M. Nastasi, *Mat. Sci. Eng. A*, in press.
- [5] N. Yu, T.E. Levine, K.E. Sickafus, M.A. Nastasi, J.N. Mitchell, C.J. Maggiore, C.R. Evans, M.G. Hollander, J.R. Tesmer, W.J. Weber, J.W. Mayer, *Nucl. Instr. and Meth. B* 118 (1996) 766.
- [6] J.F. Ziegler, J.P. Biersack, U. Littmark, *The Stopping and Range of Ions in Solids*, Pergamon Press, New York, 1985.
- [7] J.N. Mitchell, N. Yu, R. Devanathan, K.E. Sickafus, M.A. Nastasi, G.L. Nord, Jr., *Nucl. Instr. and Meth. B* 127/128 (1997) 629.
- [8] C.J. Wetteland, V. Gopalan, J.N. Mitchell, T. Hartmann, K.E. Sickafus, M.A. Nastasi, C.J. Maggiore, J.R. Tesmer, T.E. Mitchell, *Mat. Res. Soc. Proc.* 504, in press.
- [9] L.M. Wang, R.C. Ewing, *Mat. Res. Soc. Bull.* 17 (1992) 38.
- [10] D. Andrault, M.A. Bouhifd, J.P. Itié, P. Richet, *Phys. Chem. Mineral.* 22 (1995) 99.
- [11] H.M. Naguib, R. Kelly, *Radiat. Eff.* 25 (1975) 1.
- [12] L. Pauling, *J. Amer. Chem. Soc.* 49 (1927) 765.